CONFERENCE PRE-PRINT

PROGRESS TOWARDS LARGE-EDDY SIMULATION OF MULTIPHASE CONJUGATE HEAT TRANSFER IN A HYPERVAPOTRON

K. A. Damm United Kingdom Atomic Energy Authority Culham, United Kingdom Email: kyle.damm@ukaea.uk

M. Falcone United Kingdom Atomic Energy Authority Culham, United Kingdom

R. W. Eardley-Brunt United Kingdom Atomic Energy Authority Culham, United Kingdom

A. Dubas United Kingdom Atomic Energy Authority Culham, United Kingdom

A. Davis United Kingdom Atomic Energy Authority Culham, United Kingdom

Abstract

Effective management of high heat fluxes is critical for sustained tokamak operation. To address this challenge, hypervapotrons have been employed as cooling devices in plasma-facing components, including the first wall, as well as in auxiliary systems such as neutral beam injectors. Previous computational studies of hypervapotrons have primarily adopted Reynolds-Averaged Navier-Stokes (RANS) turbulence models. However, numerical predictions of recirculating cavity flows can be highly sensitive to the specific RANS model employed, leading to uncertainty in their predictive capability. Large-Eddy Simulation (LES) provides a higher-fidelity alternative capable of capturing finer-scale turbulence interactions, but its application to multiphase flow and conjugate heat transfer (CHT) in hypervapotrons remains limited. Motivated by this gap in understanding the relative accuracy of RANS and LES models, the paper presents progress towards developing the capability to perform LES of multiphase CHT in a hypervapotron within the open-source Cardinal multiphysics application. Within Cardinal, the MOOSE heat conduction module is coupled with the NekRS computational fluid dynamics solver, providing a high-fidelity framework for conjugate heat transfer modelling. At present, a key limitation of the framework is that NekRS supports only single-phase flow, though efforts are ongoing to implement a multiphase capability. While these extensions are under active development, the focus of the paper is on the first stage of this effort: validating Cardinal for CHT simulations under hypervapotron-relevant conditions in the single-phase convective regime. To this end, CHT simulations of a canonical hypervapotron model are performed using both RANS and LES turbulence models, with validation against experimental data and assessment of their relative predictive capability. Although only initial progress is reported here, the broader project aims to improve understanding of hypervapotron thermal-hydraulic behaviour across all operational regimes.

1. INTRODUCTION

Effective management of high heat fluxes in tokamak reactors presents a significant challenge crucial to their sustained operation. One solution is the utilisation of specialised high-heat-flux devices, such as the hypervapotron, which play a vital role in several components of a tokamak, including the first wall, neutral beam injectors, and

divertor systems [1]. These devices consist of ducts with repeating cavity structures, sometimes accompanied by longitudinal slots, designed to dissipate intense surface heat loads. The cavities disrupt the coolant flow and enhance local mixing, thereby improving heat transfer (see Fig. 1). Depending on the magnitude of the applied heat flux, three operational regimes can be identified: a convective regime, which occurs at sufficiently low heat fluxes where no boiling is present and heat transfer is governed by forced-convection; a nucleate boiling regime, in which localised wall regions exceed the boiling temperature, leading to nucleate boiling and an increase in heat transfer capacity; and a critical heat flux regime, where a vapour film forms on sections of the surface, reducing the local heat transfer coefficient and limiting overall performance. Reliable prediction of hypervapotron performance across its operational regimes therefore necessitates multiphase flow and boiling heat transfer models. A detailed discussion of hypervapotron applications in nuclear fusion reactors can be found in the dissertation by Milnes [2].

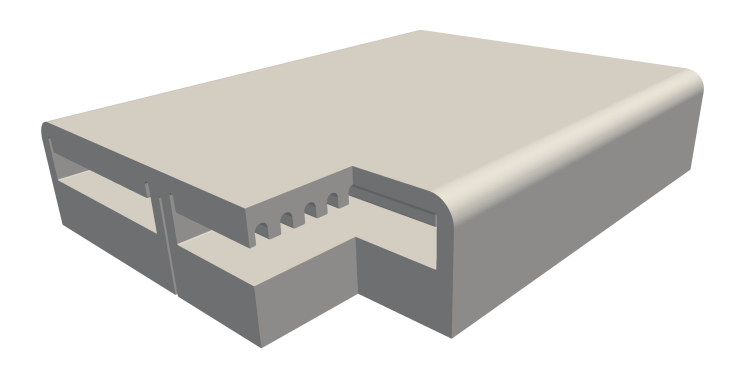


FIG. 1. 3D rendering of a representative hypervapotron geometry, illustrating the repeating cavity structure.

Despite their widespread use in the fusion community, simulations of hypervapotrons have predominantly adopted Reynolds–Averaged Navier–Stokes (RANS) turbulence models [3]. However, RANS models, particularly eddy-viscosity formulations, often perform poorly in separated, highly unsteady cavity flows, raising concerns about their applicability to hypervapotron simulations [4]. Indeed, different RANS turbulence models have been shown to produce markedly different predictions of cavity shear-layer dynamics and core recirculation, leading to uncertainty in their predictive capability [5, 6]. These shortcomings can propagate into erroneous wall heat-flux distributions and, in turn, inaccurate solid temperature fields. As a higher-fidelity alternative, Large–Eddy Simulation (LES), which explicitly captures finer-scale turbulence dynamics (compared with RANS), is commonly employed as a benchmark for assessing and calibrating RANS predictions [7]. Within the hypervapotron literature, however, LES efforts have thus far been limited mainly to the single-phase forced-convection regime [8], leaving the nucleate-boiling and critical-heat-flux regimes comparatively unexplored. Extending LES to these boiling regimes would enable resolution of the turbulence and phase-change heat transfer needed to evaluate RANS accuracy and to advance model development for design and qualification.

Motivated by this gap in understanding the relative accuracy of RANS and LES models, the paper presents progress towards LES of multiphase conjugate heat transfer (CHT) in a hypervapotron. To achieve this, the work employs the Cardinal framework [9], which integrates the MOOSE heat conduction module [10] with the NekRS high-order computational fluid dynamics (CFD) solver [11]. At present, a key limitation of the framework is that NekRS supports only single-phase flow, though efforts are ongoing to implement a multiphase capability. While the multiphase model in NekRS remains under development [12], this work lays the foundation by validating Cardinal's CHT capability for hypervapotron-relevant single-phase convection. Specifically, RANS and LES simulations of a canonical hypervapotron geometry are performed and benchmarked against the well-characterised experiment of Ciric et al. [13], which has served as a reference in numerous modelling studies [5, 6, 3, 14, 15, 16, 17, 18, 19, 20]. The remainder of this paper is organised as follows: Section 2 describes the formulation of the CHT solver, Section 3 presents validation against the Ciric et al. experiment, and Section 4 summarises conclusions and outlines directions for future development.

2. COMPUTATIONAL METHODOLOGY

This work employs Cardinal [9], a stand-alone application built on the open-source MOOSE (Multiphysics Object Oriented Simulation Environment) framework [10], which integrates the open-source Monte Carlo neutron trans-

port code OpenMC [21] with the open-source spectral element CFD solver NekRS [11]. MOOSE is a scalable finite element framework that offers a broad suite of physics modules, including heat conduction, structural mechanics, and thermo-mechanics. In the present analyses, Cardinal is used to couple NekRS with the MOOSE heat conduction module, thereby enabling thermal–hydraulic modelling through conjugate heat transfer simulations. The remainder of this section introduces the individual solvers employed in this study, summarises their governing equations, and describes the coupling strategy adopted between the different physical domains.

2.1. Fluid-Solid Coupling

In conjugate heat transfer problems, achieving stable coupling between the fluid and solid domains is particularly important when their characteristic thermal response times differ significantly. Several partitioned coupling strategies have been proposed, as reviewed by Verstraete et al. [22]. Following the work of Giles [23], we adopt the flux-forward temperature-back (FFTB) and the related heat-transfer-coefficient–forward temperature-back (hFTB) strategies in this study. In these methods, the fluid solver first runs with a fixed temperature boundary condition provided by the solid. The resulting heat flux (or heat transfer coefficient) along the shared boundary is then passed to the solid solver, which applies it as a fixed flux (or convective flux) boundary condition to compute the updated boundary temperature. We note that, during these solves, the heat flux and temperature boundary conditions are held constant in time but may vary spatially. This process is repeated iteratively to advance the simulation in time. In this framework, the fluid and solid domains are considered weakly or loosely coupled. For additional details on the transfer of information between the fluid and solid domains, including interpolation procedures, the reader is referred to the Cardinal online tutorials [24].

2.2. Solid Solver

In the MOOSE heat conduction module, the transient heat conduction equation is expressed as

$$\rho_s C_{p,s} \frac{\partial T_s}{\partial t} - \nabla \cdot (\kappa_s \nabla T_s) = \dot{q}_s, \tag{1}$$

where ρ_s is the material density [kg m⁻³], c_p the specific heat capacity [J kg⁻¹K⁻¹], T_s the solid temperature [K], t the time [s], κ_s the thermal conductivity [W m⁻¹K⁻¹], and \dot{q}_s the volumetric heat source term [W m⁻³]. The first term, $\rho_s C_{p,s} \frac{\partial T_s}{\partial t}$, represents the transient storage of thermal energy, while the second term, $-\nabla \cdot (\kappa_s \nabla T_s)$, describes heat conduction according to Fourier's law. In this work no volumetric heat source is considered, hence $\dot{q}_s = 0$.

As outlined above, various boundary conditions can be prescribed at the fluid–solid interface. For the FFTB approach, a Neumann condition prescribes a fixed-in-time but spatially varying heat flux along the shared boundary $\partial\Omega_{fs}$,

$$-\kappa_s \nabla T_s \cdot \mathbf{n} = q''(\mathbf{x}), \quad \mathbf{x} \in \partial \Omega_{fs}, \tag{2}$$

where $q''(\mathbf{x})$ is the imposed surface heat flux distribution and \mathbf{n} the outward unit normal vector. Alternatively, for the hFTB approach, a Robin (or convective) condition relates the normal heat flux to the temperature difference between the surface and the bulk fluid,

$$-\kappa_s \nabla T_s \cdot \mathbf{n} = h(\mathbf{x}) \left(T_s(\mathbf{x}) - T_\infty \right), \quad \mathbf{x} \in \partial \Omega_{fs}, \tag{3}$$

where $h(\mathbf{x})$ is the spatially varying convective heat transfer coefficient, $T_s(\mathbf{x})$ the local surface temperature, and T_{∞} the bulk fluid temperature adjacent to the boundary.

For steady-state analyses, the transient term is omitted by setting $\rho_s C_{p,s} \frac{\partial T_s}{\partial t} = 0$, and the solid temperature field is solved to a steady-state at each iteration. In contrast, when transient thermal evolution is of interest, the full formulation including the temporal term must be solved; this is also required when the solid is subject solely to Neumann boundary conditions, which render the steady-state problem ill-posed.

2.3. Fluid Solver

In this study, incompressible turbulent flow is modelled using the spectral element solver NekRS, employing both RANS and LES turbulence models. The governing RANS equations for incompressible flow comprise the continuity equation,

$$\nabla \cdot \mathbf{u} = 0,\tag{4}$$

the momentum equation,

$$\rho_f \left(\frac{\partial \mathbf{u}}{\partial t} + \mathbf{u} \cdot \nabla \mathbf{u} \right) = -\nabla P + \nabla \cdot \left[(\mu_f + \mu_T) \nabla \mathbf{u} \right], \tag{5}$$

and the energy equation,

$$\rho_f C_{p,f} \left(\frac{\partial T_f}{\partial t} + \mathbf{u} \cdot \nabla T_f \right) = \nabla \cdot \left[(\kappa_f + \kappa_T) \nabla T_f \right]. \tag{6}$$

The $k-\tau$ turbulence model [25, 26, 27, 28] is employed, which introduces additional transport equations for both the turbulent kinetic energy k and the inverse specific dissipation rate. To account for turbulent heat transfer, the model employs a constant turbulent Prandtl number, linking the turbulent viscosity μ_T to the effective thermal conductivity κ_T ,

$$Pr_T \equiv \frac{\mu_T C_{p,f}}{\kappa_T}. (7)$$

For the present work we assume $Pr_T=0.9$. Here, ${\bf u}$ is the velocity vector [m s⁻¹], ρ_f the fluid density [kg m⁻³], P the pressure [Pa], μ_f the laminar dynamic viscosity [Pa s], and μ_T the turbulent viscosity [Pa s]. The isobaric specific heat capacity is denoted by $C_{p,f}$ [J kg⁻¹ K⁻¹], T_f is the fluid temperature [K], κ_f the laminar thermal conductivity [W m⁻¹ K⁻¹], and κ_T the turbulent thermal conductivity [W m⁻¹ K⁻¹]. The turbulent kinetic energy k has units [m² s⁻²], and the inverse specific dissipation rate τ has units [s].

In the LES approach, unresolved scales are represented by an additional high-pass filtering term that modifies the Navier–Stokes equations. The governing LES equations for incompressible flow comprise the continuity equation,

$$\nabla \cdot \mathbf{u} = 0, \tag{8}$$

the filtered momentum equation,

$$\rho_f \left(\frac{\partial \mathbf{u}}{\partial t} + \mathbf{u} \cdot \nabla \mathbf{u} \right) = -\nabla P + \nabla \cdot (\mu_f \nabla \mathbf{u}) - \chi \rho_f \left(\mathbf{u} - G \mathbf{u} \right), \tag{9}$$

and the filtered energy equation,

$$\rho_f C_{p,f} \left(\frac{\partial T_f}{\partial t} + \mathbf{u} \cdot \nabla T_f \right) = \nabla \cdot (\kappa_f \nabla T_f) - \chi \rho_f C_{p,f} \left(T_f - G T_f \right). \tag{10}$$

For notational simplicity, we drop the tilde notation and take all variables to represent filtered quantities. The operator G acts as an element-wise low-pass filter implemented via convolution, while χ is a user-specified coefficient controlling the filter strength. For the present simulations, we set $\chi=10.0$ and restrict the filter action to the highest polynomial mode in each element. Further details on this method can be found in the work by Stolz et al. [29].

3. MODEL VALIDATION

This section presents results from a preliminary validation study of the conjugate heat transfer solver described in Section 2. Model validation is essential for establishing that the governing equations adequately capture the relevant physical phenomena. In this initial stage, we evaluate the solver's capability to predict the temperature distribution within the solid walls of a hypervapotron, using water as the working fluid and applying a prescribed heat flux on the external surface. To this end, conjugate heat transfer simulations of a canonical hypervapotron geometry are performed and compared against the well-characterised experiment of Ciric et al. [13].

3.1. Experiment Description

The simulations in this section aim to replicate the experimental campaign reported by Ciric et al. [13]. At JET's Neutral Beam Test Bed, hydrogen beam experiments were conducted on a full-scale Box Scraper hypervapotron prototype. The test configuration subjected the entire element to high heat fluxes while varying both beam power density and cooling water velocity, enabling measurements of surface temperatures and overall cooling performance. The applied power densities encompassed the full range of hypervapotron operating regimes, from single-phase conditions through the onset of boiling. Given the current limitation of single-phase modelling in NekRS, we focus here on the lowest power density of $3.8\,\mathrm{MW\,m^{-2}}$ and a fluid velocity of $U=4.0\,\mathrm{m\,s^{-1}}$, which is believed to lie near the upper boundary of single-phase operation, based on the computational results of Milnes [2].

For all simulations presented in this work, water is modelled with constant thermophysical properties evaluated at the inflow temperature of $50^{\circ}\mathrm{C}$ (as discussed in the following section): density $\rho=9.970\times10^{2}~\mathrm{kg}~\mathrm{m}^{-3}$, dynamic viscosity $\mu=5.474\times10^{-4}~\mathrm{Pa}~\mathrm{s}$, specific heat capacity $C_p=4.186\times10^{3}~\mathrm{J}~\mathrm{kg}^{-1}~\mathrm{K}^{-1}$, and thermal conductivity $\kappa=6.406\times10^{-1}~\mathrm{W}~\mathrm{m}^{-1}~\mathrm{K}^{-1}$. For the solid domain, the CuCrZr material is modelled with constant properties: density $\rho=8.920\times10^{3}~\mathrm{kg}~\mathrm{m}^{-3}$, specific heat capacity $C_p=3.81\times10^{2}~\mathrm{J}~\mathrm{kg}^{-1}~\mathrm{K}^{-1}$, and thermal conductivity $\kappa=3.30\times10^{2}~\mathrm{W}~\mathrm{m}^{-1}~\mathrm{K}^{-1}$.

3.2. Simulation Setup

For the RANS simulations, we follow a setup similar to that described by Milnes [2], where two cavities are simulated around the midpoint of the hypervapotron. The inflow temperature at this location is not directly available and must be approximated; following Milnes [2], we estimate it to be 50°C to account for the bulk heating in the upstream half of the hypervapotron. In the RANS simulations, the fluid domain is prescribed with an inflow boundary condition specifying velocity, temperature, and the turbulence variables k and τ (assuming a turbulence intensity of 5%), a zero-gradient outflow boundary condition at the outlet, and no-slip conditions on the walls. In the LES simulations, the fluid domain consists of a single cavity element with periodic boundary conditions at the inlet and outlet and no-slip conditions at the walls. For both RANS and LES cases, the solid domain is subjected to an imposed surface heat flux of 3.8 MW m⁻² on the top wall, along with the coupled fluid-solid boundary conditions described in Section 2.2; all remaining boundaries are assumed to be adiabatic, consistent with operation of the hypervapotron in a vacuum chamber. The approximate midpoint temperature was also used to initialise the fluid domain in both the RANS and LES simulations. The computational meshes were generated using Coreform Cubit 2025.8 [30]. For the RANS simulations, the mesh consisted of approximately 350,000 solid tetrahedral elements and 1.2 million fluid hexahedral elements. Each fluid element employed a tensor-product polynomial basis of order N=3 in three spatial dimensions, corresponding to $(N+1)^3=64$ grid points per element. For the LES simulations, the mesh consisted of approximately 225,000 solid tetrahedral elements and 800,000 fluid hexahedral elements, with a tensor-product polynomial basis of order N=5, corresponding to $(N+1)^3=216$ grid points per element. In both cases, the fluid meshes achieved an average y^+ of approximately 1. A preliminary grid sensitivity assessment was performed. For the solid domains, the element size was reduced by roughly a factor of two in each spatial direction. For the fluid domains, simulations were repeated with a polynomial order increased by one relative to the baseline case. The predicted surface temperature differences were within a few percent. However, a formal grid convergence study is still ongoing, and the results presented here should be regarded as preliminary.

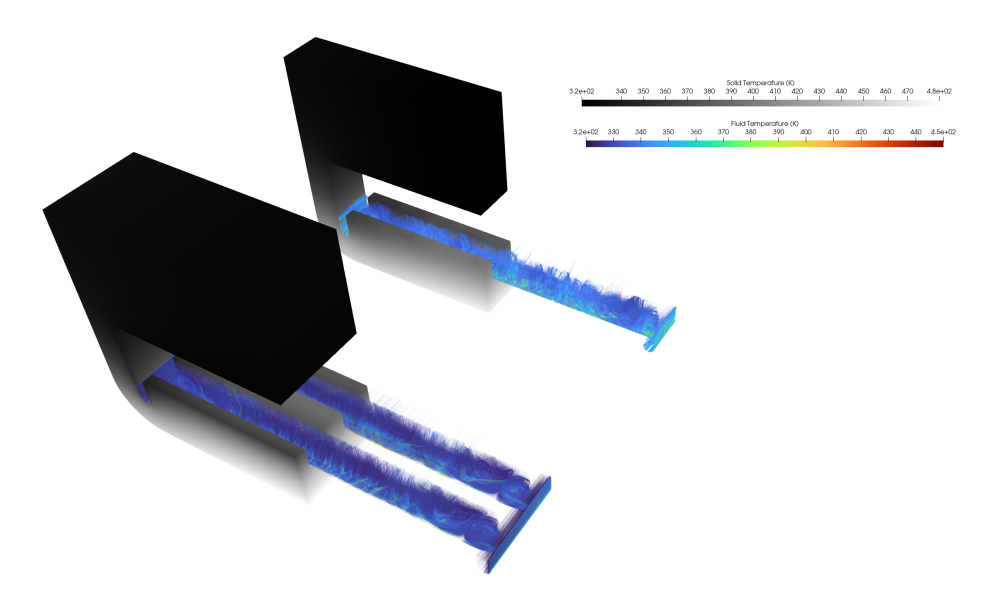


FIG. 2. Fluid-solid solution: RANS (foreground) and LES (background). Solid temperatures are shown in grayscale, while fluid streamlines are coloured by local temperature.

3.3. Results

An example of the coupled fluid–solid simulation results is shown in Figure 2, where the solid temperature field is visualised alongside fluid streamlines in the cavity region, coloured by the local fluid temperature.

In the experiments of Ciric et al. [13], the surface temperature rise was reported under the assumption that the initial solid temperature was below 50°C. However, personal correspondence with researchers familiar with the JET experiments indicates that the initial solid temperature was likely closer to 20°C. To account for this uncertainty, the computed surface temperature rise is presented with error bars reflecting these upper and lower bounds of the initial solid temperature. The predicted surface temperature rise from both the RANS and LES simulations is compared with the experimental data in Figure 3. Both approaches show reasonable agreement with the measurements within the uncertainty of the initial solid temperature. The LES results predict slightly higher surface temperatures than the RANS results. This can be attributed to the periodic boundary conditions employed in the LES simulations: fluid heated within the cavity mixes with the bulk stream, exits the domain, and then re-enters, leading to progressive heating, as evident in Figure 2. This reduces the driving temperature difference between the solid and fluid, thereby diminishing convective heat transfer and resulting in higher solid temperatures. In general, both the RANS and LES simulations predict a larger surface temperature rise than reported in the experiments. One possible explanation is that, as shown in Figure 2, regions of the fluid domain exceed the boiling point of water. If multiphase effects were included, the effective heat transfer would likely increase due to nucleate boiling, which may explain why the simulations slightly overpredict the measured wall temperatures. However, in the absence of experimental error bars, definitive conclusions cannot be drawn.

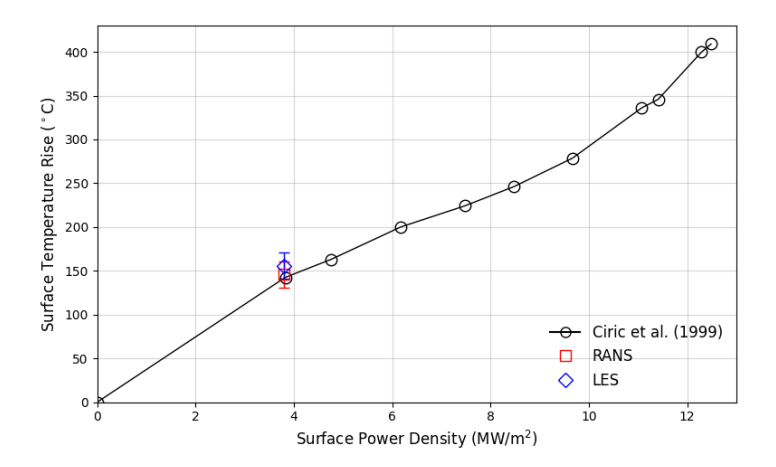


FIG. 3. Comparison of surface temperature rise versus surface power density, showing experimental data from Ciric et al. [13] alongside predictions from RANS and LES simulations.

Preliminary comparisons of the bulk flow features between the RANS solutions and the time-averaged LES results indicate broadly similar large-scale structures. Sensitivity studies on the inlet value of τ were also performed; however, only a modest change in the predicted surface temperature rise was observed, on the order of a few kelvin. Further analysis of bulk flow features is ongoing as part of the grid convergence study, along with an exploration of alternative LES setups in which the fluid temperature is initialised with the reported inlet temperature of the hypervapotron. Results from these investigations are pending.

4. CONCLUSION

This work represents the first step toward LES of multiphase CHT in a hypervapotron. We have validated the Cardinal framework, coupling NekRS and MOOSE, for the single-phase convective regime of the JET hypervapotron experiments. RANS and LES simulations at $3.8\,\mathrm{MW\,m^{-2}}$ and $U=4.0\,\mathrm{m\,s^{-1}}$ reproduced the reported surface temperature rise within the bounds of the initial solid temperature uncertainty, with LES predicting slightly higher wall temperatures than RANS, consistent with the modelling choices discussed. Ongoing work is focused on porting the multiphase algorithm from Nek5000 [12] into NekRS and implementing phase-change boiling models. These efforts aim to build a framework for benchmarking turbulence models and advancing predictive simulations of hypervapotron performance in high-heat-flux fusion applications.

ACKNOWLEDGEMENTS

This work was supported by the Fusion Futures Programme, announced by the UK Government in October 2023 to provide holistic support for the development of the fusion sector. The authors also acknowledge the use of

resources provided by the Cambridge Service for Data Driven Discovery (CSD3). Finally, we gratefully thank April Novak of the University of Illinois Urbana–Champaign and fellow contributors to the open-source Cardinal project for their efforts in developing and maintaining the software employed in this work.

REFERENCES

- [1] Raffray, A. et al. "High heat flux components—Readiness to proceed from near term fusion systems to power plants". In: *Fusion Engineering and Design* 85.1 (2010), pp. 93–108. ISSN: 0920-3796. DOI: https://doi.org/10.1016/j.fusengdes.2009.08.002.
- [2] Milnes, J. "Computational modelling of the HyperVapotron cooling technique for nuclear fusion applications". PhD thesis. Cranfield University, 2010. URL: https://dspace.lib.cranfield.ac.uk/items/3cc32b81-f04c-4f6b-a370-97b2bd409b24.
- [3] Smolík, V. "HyperVapotron high heat flux cooling technology". Master's thesis. Czech Technical University in Prague, 2022. DOI: https://doi.org/10.13140/RG.2.2.20940.08328.
- [4] Pope, S. B. *Turbulent Flows*. Cambridge: Cambridge University Press, 2000. ISBN: 978-0521598866. DOI: 10.1017/CB09781316179475.
- [5] Milnes, J. and Drikakis, D. "Qualitative assessment of RANS models for Hypervapotron flow and heat transfer". In: *Fusion Engineering and Design* 84.7 (2009). Proceeding of the 25th Symposium on Fusion Technology, pp. 1305–1312. ISSN: 0920-3796. DOI: https://doi.org/10.1016/j.fusengdes. 2008.12.004.
- [6] Milnes, J., Burns, A., and Drikakis, D. "Computational modelling of the HyperVapotron cooling technique". In: Fusion Engineering and Design 87.9 (2012), pp. 1647–1661. ISSN: 0920-3796. DOI: https://doi.org/10.1016/j.fusengdes.2012.06.014.
- [7] Sagaut, P. Large Eddy Simulation for Incompressible Flows: An Introduction. 3rd ed. Scientific Computation. Berlin, Heidelberg: Springer, 2006. DOI: 10.1007/b137536.
- [8] Mallick, Z. "Computational modelling of cavity arrays with heat transfer using implicit large eddy simulations". PhD thesis. Cranfield University, 2010. URL: https://dspace.lib.cranfield.ac.uk/items/50b25f03-2bb6-45e6-a2f8-6d4d5cb4b649.
- [9] Novak, A. et al. "Coupled Monte Carlo and thermal-fluid modeling of high temperature gas reactors using Cardinal". In: *Annals of Nuclear Energy* 177 (2022), p. 109310. ISSN: 0306-4549. DOI: https://doi.org/10.1016/j.anucene.2022.109310.
- [10] Giudicelli, G. et al. "3.0 MOOSE: Enabling massively parallel multiphysics simulations". In: *SoftwareX* 26 (2024), p. 101690. ISSN: 2352-7110. DOI: https://doi.org/10.1016/j.softx.2024.101690.
- [11] Fischer, P. et al. "NekRS, a GPU-accelerated spectral element Navier-Stokes solver". In: *Parallel Computing* 114 (2022), p. 102982. ISSN: 0167-8191. DOI: https://doi.org/10.1016/j.parco.2022.102982.
- [12] Saini, N. et al. "A High Order Continuous Galerkin Spectrally Stabilized Level-Set Approach for Incompressible Two-Phase Flows". In: SSRN Preprint (Jan. 2025). Preprint. DOI: 10.2139/ssrn.5397463.
- [13] Ciric, D. et al. "Design issues and fatigue lifetime of hypervapotron elements of the JET neutral beam injectors". In: 18th IEEE/NPSS Symposium on Fusion Engineering. Symposium Proceedings (Cat. No.99CH37050). 1999, pp. 407–410. DOI: https://doi.org/10.1109/FUSION.1999.849867.
- [14] Smolik, V. et al. "Hypervapotron High Heat Flux Cooling Numerical and Experimental Study". In: *Proceedings of the 10th International Conference on Fluid Flow, Heat and Mass Transfer (FFHMT'23)*. Paper No. 181. Ottawa, Canada: Avestia Publishing, 2023, pp. 181-1–181-6. DOI: https://doi.org/10.11159/ffhmt23.181.
- [15] Domalapally, P. K. "Computational Thermal Fluid Dynamic Analysis of Cooling Systems for Fusion Reactor Components". Ph.D. thesis. Turin, Italy: Politecnico di Torino, 2013. DOI: 10.6092/polito/porto/2514474.
- [16] Domalapally, P. "Assessment of hypervapotron heat sink performance using CFD under DEMO relevant first wall conditions". In: *Fusion Engineering and Design* 109-111 (2016). Proceedings of the 12th International Symposium on Fusion Nuclear Technology-12 (ISFNT-12), pp. 109-113. ISSN: 0920-3796. DOI: https://doi.org/10.1016/j.fusengdes.2016.03.044.

- [17] Domalapally, P. and Subba, F. "Computational thermal fluid dynamic analysis of Hypervapotron heat sink for high heat flux devices application". In: *Fusion Engineering and Design* 98-99 (2015). Proceedings of the 28th Symposium On Fusion Technology (SOFT-28), pp. 1267–1270. ISSN: 0920-3796. DOI: https://doi.org/10.1016/j.fusengdes.2015.02.017.
- [18] Písek, V. "Ověření aplikovatelnosti CFD metodik pro výpočty podchlazeného varu". Master's thesis. Prague: České vysoké učení technické v Praze, Fakulta strojní, June 10, 2016. URL: http://hdl.handle.net/10467/66240.
- [19] Pitoňák, V. "Studie podchlazeného varu v hypervapotronu". Master's thesis. Prague: České vysoké učení technické v Praze, Fakulta strojní, Jan. 11, 2017. URL: http://hdl.handle.net/10467/70909.
- [20] Gleitz, M. et al. "Design of Experimental Device for Testing of Subcooled Flow Boiling". In: *Engineering Mechanics 26th International Conference* (Brno, Czech Republic, Nov. 24–25, 2020). Brno University of Technology, Institute of Solid Mechanics, Mechatronics and Biomechanics, 2020, pp. 150–153. ISBN: 978-80-214-5896-3. DOI: https://doi.org/10.21495/5896-3-150.
- [21] Romano, P. K. et al. "OpenMC: A state-of-the-art Monte Carlo code for research and development". In: Annals of Nuclear Energy 82 (2015), pp. 90–97. ISSN: 0306-4549. DOI: https://doi.org/10.1016/j.anucene.2014.07.048.
- [22] Verstraete, T. and Van den Braembussche, R. "A Novel Method for the Computation of Conjugate Heat Transfer with Coupled Solvers". In: *Proceedings of International Symposium on Heat Transfer in Gas Turbine Systems.* Begel House Inc. 2009, pp. 1–17. DOI: https://doi.org/10.1615/ICHMT.2009.HeatTransfGasTurbSyst.570.
- [23] Giles, M. B. "Stability analysis of numerical interface conditions in fluid-structure thermal analysis". In: *International Journal for Numerical Methods in Fluids* 25.4 (1997), pp. 421–436. DOI: https://doi.org/10.1002/(SICI)1097-0363(19970830)25:4<421::AID-FLD557>3.0.CO;2-J.
- [24] Novak, A. J. Conjugate Heat Transfer Coupling of NekRS and MOOSE Tutorial. Cardinal, Argonne National Laboratory. 2025. URL: https://cardinal.cels.anl.gov/tutorials/cht.html (visited on 09/03/2025).
- [25] Tomboulides, A. et al. "A robust spectral element implementation of the *k*–*τ* RANS model in Nek5000/NekRS". In: *International Journal of Heat and Fluid Flow* 112 (2025), p. 109679. ISSN: 0142-727X. DOI: https://doi.org/10.1016/j.ijheatfluidflow.2024.109679.
- [26] Speziale, C. G., Abid, R., and Anderson, E. C. "Critical evaluation of two-equation models for near-wall turbulence". In: *AIAA Journal* 30.2 (1992), pp. 324–331. DOI: https://doi.org/10.2514/3.10922.
- [27] Benton, J., Kalitzin, G., and Gould, A. "Application of two-equation turbulence models in aircraft design". In: *34th Aerospace Sciences Meeting and Exhibit*. AIAA Paper 96-0327. Reno, NV, USA: American Institute of Aeronautics and Astronautics, 1996. DOI: https://doi.org/10.2514/6.1996-327.
- [28] Kok, J. C. and Spekreijse, S. P. *Efficient and Accurate Implementation of the k–ω Turbulence Model in the NLR Multi-Block Navier–Stokes System.* Technical Report NLR-TP-2000-144. National Aerospace Laboratory (NLR), 2000. URL: http://hdl.handle.net/10921/822.
- [29] Stolz, S., Adams, N. A., and Kleiser, L. "An approximate deconvolution model for large-eddy simulation with application to incompressible wall-bounded flows". In: *Physics of Fluids* 13.4 (Apr. 2001), pp. 997–1015. ISSN: 1070-6631. DOI: https://doi.org/10.1063/1.1350896.
- [30] Coreform LLC. Coreform Cubit 2025.8. https://coreform.com/products/coreform-cubit/. Version 2025.8, Orem, Utah, USA. 2025.